Geomechanics and Engineering, *Vol. 30, No. 6 (2022) 565-577*
https://doi.org/10.12989/gae.2022.30.6.565

Investigation of three-dimensional deformation mechanisms of box culvert due to adjacent deep basement excavation in clays

Fanmin Bu[1], Wenrui Yu*[1], Li Chen[2] and Erlu Wu[3]

[1]*CCCC Fourth Highway (Beijing) Highway Test Checking Technology Co., Ltd, Beijing 101107, China*
[2]*Nanjing Gongda Construction Technology Co., Ltd, Nanjing, Jiangsu 210009, China*
[3]*Key Laboratory of Ministry of Education for Geomechanics and Embankment Engineering, Hohai University, Nanjing, Jiangsu 210024, China*

(*Received July 3, 2022, Revised August 15, 2022, Accepted September 8, 2022*)

Abstract. In this study, a series of three-dimensional numerical parametric study was conducted to investigate deformation mechanisms of an existing box culvert due to an adjacent multi-propped basement excavation in clays. Field measurements from an excavation case history are first used to calibrate a baseline Hardening Soil Small Strain (HS-small) model, which is subsequently adopted for parametric study. Results indicate that the basement-box culvert interaction along the basement centerline can be considered as a plane strain condition when the length of excavation (L) reaches 14 H_e (i.e., final excavation depth). If a plane strain condition (i.e., L/H_e=12.0) is assumed for analyzing the basement-box culvert interaction of a short excavation (i.e., L/H_e=2.0), the maximum settlement and horizontal movement of the box culvert are overestimated significantly by up to 15.7 and 5.1 times, respectively. It is also found that the deformation of box culvert can be greatly affected by the basement excavation if the distance between the box culvert and retaining wall is less than 1.5 H_e. The induced deformation in the box culvert can be dramatically reduced by improving the ground inside the excavation or implementing other precautionary measures. For example, by adding jet grouting columns within the basement and installing an isolation wall behind the retaining structures, the maximum settlements of box culvert are shown to reduce by 37.2% and 13.4%, respectively.

Keywords: basement excavation; box culvert; horizontal movement; settlement; three-dimensional

1. Introduction

In congested urban cities, it is not uncommon to construct basements for high-rise buildings in close proximity to existing utilities (e.g., pipelines) (O'Rourke *et al*. 2001, Shi *et al*. 2022a), foundations (e.g., Ng *et al*. 2004, Liyanapathirana and Nishanthan 2016, Zhang *et al*. 2019, Soomro *et al*. 2021, Yang *et al*. 2022, Fang *et al*. 2022, Shi *et al*. 2022b), and other structures (e.g., Devriendt *et al*. 2010, Ng *et al*. 2013, Kouretzis *et al*. 2014, Fong *et al*. 2014, Shi *et al*. 2015a) such as box culvert. Excavation works for basement construction can inevitably cause disturbances in the ground and induce additional stresses and deformations in existing structures, which could possibly affect the serviceability and ultimate capacity of adjacent structures. For example, Wang *et al*. (2019) reported the collapse of a 13-storey high-rise residential building in Shanghai soft clay due to a 4.6m deep excavation at 7m away from the soil-nailed wall. Therefore, it is imperative to have a sound understanding about potential deformation mechanisms of any structures lying within the influence zone of an excavation, particularly when the in-situ soils have low undrained shear strength and high compressibility.

In literature, many studies (e.g., Ng *et al*. 2012, Shi *et al*. 2018, Hsiung *et al*. 2018, Shi *et al*. 2019, Shi *et al*. 2020, Qian *et al*. 2020, Mu *et al*. 2021) have been carried out to investigate soil-structure interaction problems due to basement excavation. For example, Hsiung *et al*. (2018) reported an excavation case history in Central Jakarta and back-analyzed it using three-dimensional analysis in order to explore three-dimensional wall deformation mechanisms. Results indicate that the critical plane strain ratio (PSR) for treating a three-dimensional excavation as a two-dimensional problem is closely related to the corner effects, and a minimal distance of 50m away from corners of an excavation was required. In addition, effects of three-dimensional excavations on existing infrastructures such as tunnels have also been extensively studied over the past decades (e.g., Ng *et al*. 2012). To counterbalance or minimize the adverse effects of excavation on existing structures, Shi *et al*. (2018) carried out three-dimensional numerical analyses to evaluate countermeasures to minimize excavation-induced heaving in existing tunnels, which lay directly beneath the excavation. Extensive studies have also been carried to investigate responses of geotechnical systems subjected to soil spatial variability and stratigraphic uncertainty (e.g., Pan *et al*. 2018, Shi and Wang 2021, Nguyen and Likitlersuang 2021, Wang *et al*. 2022). Although previous studies have been devoted to investigating the deformation patterns of existing structures subjected to adjacent braced excavation, they rarely shed light on the effectiveness of various feasible precautionary in constraining or reducing induced deformations in an existing box culvert. In addition, there lacks a systematical

*Corresponding author, Ph.D.
E-mail: ceyuwenrui@163.com

Copyright © 2022 Techno-Press, Ltd.

ISSN: 2005-307X (Print), 2092-6219 (Online)

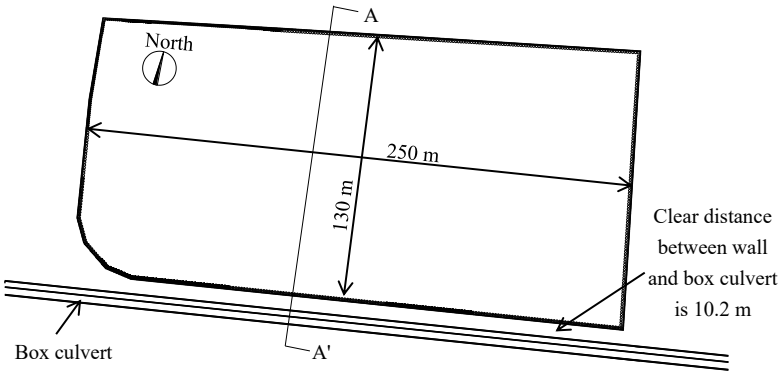

Fig. 1 Plan view of the site

and comprehensive understanding regarding critical factors (i.e., system stiffness and excavation geometry) governing the overall response of an existing structure in close proximity to a braced excavation.

To explicitly tackle the above-mentioned challenges, a series of three-dimensional numerical parametric study was conducted to investigate deformation mechanisms of an existing box culvert due to an adjacent multi-propped basement excavation in clays. The geotechnical engineering properties of soils are modelled using the Hardening Soil model with small strain stiffness and calibrated using field measurements from a case history in Nanjing. The verified numerical model is subsequently adopted to establish excavation-induced deformation mechanisms of an existing box culvert considering varied geometry of excavation, retaining wall stiffness and ground improvement measures (i.e., an isolation wall). Useful insights are gained from the numerical study. The remainder of this study is organized as follows. In Section 2, site conditions of a real excavation case history in Nanjing are briefly introduced. A 3D numerical model is established and calibrated in Section 3, and the numerical parametric analysis program is presented in Section 4. The computed results are interpreted in Section 5, followed by the summary and conclusions.

2. The site

2.1 Basement and box culvert

The site mainly comprised a deep basement for a large residential building in Nanjing, which is a coastal megacity in eastern China. In this site, the ground water table was 1.5 m below the ground surface. Fig. 1 shows the plan layout of the site. The basement was approximately rectangular and 250 m×130 m in plan. There was an existing box culvert located to the south of the basement. The box culvert was almost parallel to the long side of the basement, and the clear distance between the box culvert and basement was about 10.2 m.

Fig. 2 shows a typical elevation view of the basement along cross-section A-A' (see Fig. 1). The ground had an elevation of +7.4 m, and the final formation level of basement was -8.4 m. Thus, the final excavation depth (H_e) of the basement was 15.8 m. To reduce basement

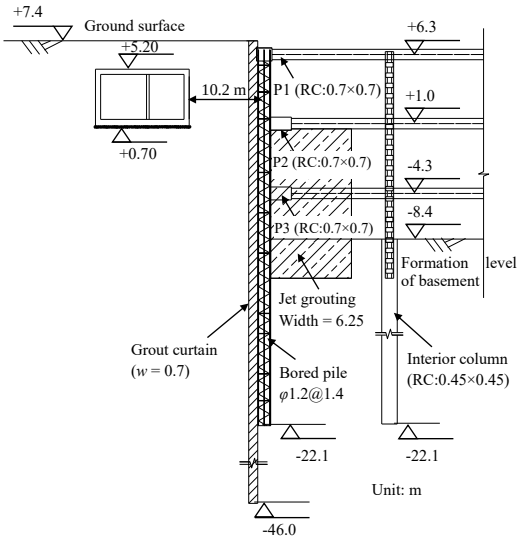

Fig. 2 Elevation view of basement and box culvert

excavation-induced adverse effects on nearby infrastructures (i.e., box culvert), a row of bored piles with a diameter of 1.2 m and a spacing of 1.4 m was constructed along the perimeter of the basement as retaining structures. In addition, three levels of concrete props, each prop with a cross-sectional area of 0.7 m×0.7 m, were installed at respective elevations of +6.3, +1.0 m and -4.3 m to restrain the lateral movement of retaining structures. The horizontal spacing between props at the same elevation was approximately 8 m. Within the basement, multiple rectangular concrete columns with a cross-sectional area of 0.45m×0.45m were constructed to balance the weight of props. The total length of interior columns was 28.75 m, which was the same as the bored pile wall. To prevent water leakages, grout curtain with a thickness of 0.7 m was constructed behind the bored pile wall. The curtain had a length of 53.4 m and penetrated 2 m into completely decomposed granite (CDG). Moreover, jet grouting columns were applied to reinforced soils within the basement, and the height and width of the jet grouting zone were 11.2 m and 6.25 m, respectively.

For the box culvert located at the side of the basement, it consisted of five concrete walls. The thicknesses of concrete walls were 0.3 m with the exception that the partition wall had a thickness of 0.2 m. The burial depth,

Table 1 Geotechnical properties of soil in this site

Soil Type	Soil Parameter					
	Depth (m)	Water content (%)	Unit weight (kN/m^3)	Constrained modulus, $E_{s1\text{-}2}$ (MPa)	Cohesion (kPa)	Fiction angle (°)
①_1 Fill	0~4.4	22.2	18.6	4.0	8.0	25.0
②_2 Soft clay	4.4~10.6	40.4	17.6	3.4	8.0	27.0
②_3 Silty clay	10.6~14.4	38.5	17.7	3.7	4.3	28.0
②_4a Silty sand	14.4~48.1	26.1	19.0	15.0	8.0	31.6
②_6a Silty clay	48.1~49.0	30.9	18.2	4.7	5.0	35.0
③_4 Gravel	49.0~50.6	24.6	19.4	100.0	20.0	35.0
⑤_1 CDG	50.6~57.4	20.0	22.7	200.0	200.0	30.0

width and height of the box culvert were 1.2 m, 14.0 m and 4.35 m, respectively. Note that the clear distance between the culvert box and retaining bored pile wall was 10.2 m, which was within the primary influence zone of ground settlement due to basement excavation (i.e., 2 H_e as reported by Hsieh and Ou (1998)). Therefore, it is anticipated that the serviceability and safety of the box culvert may be affected by the adjacent deep excavation.

2.2 Geology

The site was located at the central area of Nanjing, which was close to Yangtze and Qinghai rivers. As a result, the soil stratum in this site mainly consisted of fill, soft clay, silty clay, silty sand, gravel and completely decomposed granite (CDG). Because of relatively large excavation area on plan, the subsurface geology was not horizontal in this site. This study focused on deformation mechanisms of box culvert due to adjacent basement excavation. Thus, deformations of box culvert were significantly affected by soil properties close to the existing box culvert. For simplicity, the subsurface geology was assumed to be horizontal. Based on geological profile of soil close to box culvert, thickness of each soil layer was determined.

Table 1 summaries basic geotechnical properties of the soils at this site. The total thickness of the upper three soil layers (i.e., fill, soft clay and silty clay) was 14.4 m, underlaid by silty sand with a thickness of 33.7 m. Moreover, completely decomposed granite (CDG) was located 50.6 m below the ground surface. Two thin soil layers, namely, silty clay and gravel, lay between the silty sand and CDG. In this site, the final excavation depth of the basement was 15.8 m, indicating that excavation was mainly carried out within upper four soil layers. Moreover, the entire box culvert was buried in soft clay. Thus, performances of the basement and box culvert were expected to be greatly affected by geotechnical properties of fill, soft clay, silty clay and silty sand.

Prior to basement excavation, a series of laboratory tests was conducted to obtain geotechnical properties of each soil type at this site. By conducting one-dimensional compression test, the constrained modulus ($E_{s1\text{-}2}$) was obtained at the stress level ranging from 100 to 200 kPa. The measured constrained stiffness (i.e., E_s under a vertical stress ranging from 100 to 200 kPa) of upper four soil layers varied from 3.4 to 15.0 MPa. Based on the undrained consolidated triaxial tests, the measured friction angle and cohesion of upper four soil layers were in ranges of 4.3 ~8.0 kPa and 25.0°~31.6°, respectively.

2.3 Instrumentation

To ensure serviceability and safety of the existing box culvert during basement excavation, various instruments were installed at this site. To monitor the lateral movement of the bored pile wall due to basement excavation, inclinometers tubes were installed before concreting. The lateral wall movements were measured at 0.5 m interval. Since inclinometers only gave relative lateral movements, control marker was installed at the top of each inclinometer tube to measure the absolute lateral movement of a bored pile prior to excavation. Moreover, settlement markers were installed on the base slab of the box culvert along its longitudinal direction to monitor basement excavation-induced box culvert settlements. In total, 16 settlement markers were installed to obtain basement excavation induced settlements in the box culvert.

3. Three-dimensional numerical back-analysis

3.1 Three-dimensional numerical mesh and boundary conditions

Fig. 3 shows the three-dimensional finite element mesh used to back-analyze the field test. As shown in Fig. 1, the basement was approximately rectangular and therefore only a quarter of the basement was modelled in the numerical analysis for computational efficiency. Since the geometry of the basement was close to rectangular shape, the excavation was modelled as a rectangle for simplification. Note that the key parameter, namely excavation length along the longitudinal direction, was accurately simulated. Based on the equivalent axial and flexural stiffnesses of the columns and props, a unform spacing of the props was simulated for simplification. Obviously, the lateral wall movements due to basement excavation were controlled by axial stiffness of the props. As long as the axial stiffness of props was properly simulated, the computed results were not greatly affected by this simplification.

The bored pile wall was adopted as the primary retaining structure. Bending was the key deformation

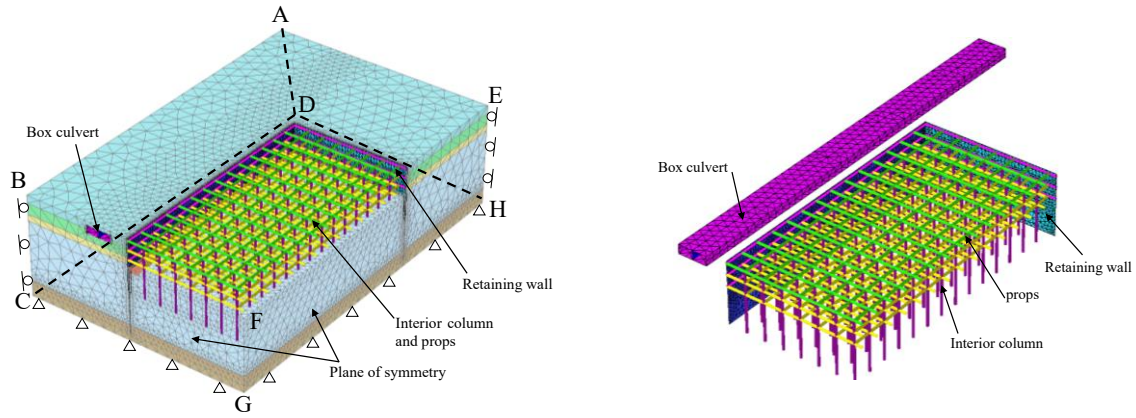

(a) Three-dimension finite element mesh (b) Retaining system and box culvert

Fig. 3 Three-dimension numerical mesh of basement-box culvert interaction

Table 2 Construction phases and sequences of the basement excavation

Phase	Construction sequences	Note
1	Construction of box culvert	Activate plate elements for box culvert
2	Construction of bored pile retaining wall, grout curtain, jet grouting, interior column	Activate plate elements for retaining structures
3	Dewatering to the elevation of +4.3 m, and soil excavated to the elevation of +5.3 m	Deactivate soil elements
4	Installing the first level of concrete props (P1) at the elevation of +6.3 m	Activate beam elements of P1
5	Dewatering to the elevation of -1.0 m, and soil excavated to the elevation of +0.0 m	Deactivate soil elements
6	Installing the second level of concrete props (P2) at the elevation of +1.0 m	Activate beam elements of P2
7	Dewatering to the elevation of -6.3 m, and soil excavated to the elevation of -5.3 m	Deactivate soil elements
8	Installing the third level of concrete props (P3) at the elevation of -4.3 m	Activate beam elements of P3
9	Dewatering to the elevation of -9.4 m, and soil excavated to the elevation of -8.4 m	Deactivate soil elements
10	Construction of concrete base slab	Activate plate elements of concrete slab

mechanisms of the bored pile wall, which was the same as continuous walls. For simplification, the bored pile wall was simulated as continuous wall in the numerical analysis. Based on equivalent flexural stiffness, the bored pile wall was modelled as a plate with an equivalent thickness of 0.8 m. Based on the fielding monitoring, Heish and Ou (1998) found that the influence zone of ground settlement behind the retaining wall due to basement excavation was 4 times of the final excavation depth (i.e., 4 H_e). In the numerical analysis, the distance between the boundary of the mesh and retaining was larger than 6 H_e. Thus, the computed movements of box culvert were not affected by the boundary conditions.

In this study, the box culver and retaining wall were simulated by shell element, while soil stratum was modelled by10 noded tetrahedron elements. For props and interior columns, beam elements were used. The three-dimensional mesh in total comprised 203214 elements and 311100 nodes. If the number of elements and nodes was increased by 100%, the difference in the maximum settlement of the box culvert was less than 2%, indicating that the current mesh density was already fine enough. Soil movements perpendicular to the planes of ABCD and ADHE were constrained both horizontally and vertically, while soil movements at the plane of CDHG were constrained in all three directions. Moreover, plane of symmetry boundary was applied to the planes of BCGF and EFGH. By using a computer with a CPU 2.7 GHz of and a ram memory of 32 G, each numerical run took about 3~ 4 fours.

3.2 Construction sequences

Table 2 summarizes construction sequences simulated in the numerical analysis. Firstly, the construction of box culvert was simulated by activating plate elements. Subsequently, bored pile wall, interior column, grout curtain and jet grouting within basement were installed. Finally, the basement excavation was carried out in four steps. For each excavation step, the ground water table within the basement was dewatered to 1.0 m below the designated excavation level before removal of soil. After soil was excavated to a target level, corresponding level of props was installed 1 m above the excavation level. Finally, concrete slabs with a thickness of 1.0 m were cast upon completion of basement excavation.

3.3 Constitutive model and model parameters

As reported by previous studies, shear strains of soils surrounding basement were commonly in a range of 0.01%

Table 3 Soil parameters for hardening soil model with small strain stiffness (HSS)

Model Parameter	Soil Type							
	①_1 Fill	②_2 Soft clay	②_3 Silty clay	②_4a Silty sand	②_6a Silty clay	③_4 Gravel	⑤_1 CDG	Cement soil
Secant modulus, E_{50}^{ref} (Mpa)	4.0	3.4	3.7	15.0	4.7	100.0	200.0	100.0
Tangent oedometric modulus, E_{oed}^{ref} (Mpa)	4.0	3.4	3.7	15.0	4.7	100.0	200.0	100.0
Unloading-reloading modulus, E_{ur}^{ref} (Mpa)	24.0	20.4	22.2	90.0	28.2	400.0	600.0	300.0
Modulus stress related power exponent, m	0.65	0.80	0.8	0.5	0.8	0.5	0.5	0.5
Effective cohesion, c' (kPa)	5.0	8.0	8.0	4.3	8.0	5.0	20	200.0
Effective friction angle, φ' (°)	30.0	25.0	27.0	31.6	28.0	35.0	35	30.0
Shear strain corresponding to initial shear modulus, $\gamma_{0.7}$ (10^{-4})	2.0	2.0	2.0	1.0	2.0	1.0	1.0	1.0
Reference initial shear modulus, G_0^{ref} (Mpa)	72.0	61.2	66.6	270.0	84.6	1200	1800	900

to 0.1% (e.g., Ng *et al*. 2009, Wong *et al*. 2014). Soil stiffness was known to degrade dramatically with increasing shear strain particularly within a small strain range. As reported by previous studies, ground movement behind the retaining wall could not accurately be predicted by simple model (i.e., Mohr-Column model and hardening soil model). The hardening soil model with small-strain stiffness (HSS) could capture the effects of shear strain on soil stiffness. By using HSS model, ground movement around the basement and structure responses were accurately computed (e.g., Zheng *et al*. 2018, Ng *et al*. 2021). The hardening soil model with small-strain stiffness (HSS) (Ardakani *et al*. 2014) was thus used to simulate basement-soil-box culvert interaction, while responses of box culvert and basement were simulated using an elastic model.

Table 3 summarizes soil parameters of the HHS model adopted in this study. There were four stiffness parameters, namely, secant modulus (E_{50}^{ref}), tangent oedometric modulus (E_{oed}^{ref}), unloading-reloading modulus (E_{ur}^{ref}) and initial shear modulus G_0^{ref}). Ideally, all those stiffness parameters should be obtained by conducting laboratory tests. In absence of direct measurements, an alternative approach was used in this study to determine soil parameters for HSS model. Note that there were well-established empirical correlations for estimating stiffness parameters with respect to constrained modulus (E_s). The adopted relationships among those stiffness parameters were as follows (e.g., Brinkgreve *et al*. 2004, Zheng *et al*. 2018, Ng *et al*. 2021)

$$E_{oed}^{ref} = E_{50}^{ref} = E_s \quad (1)$$

$$E_{ur}^{ref} = (2\sim6)E_{50}^{ref} \quad (2)$$

$$G_0^{ref} = 3E_{ur}^{ref} \quad (3)$$

Based on the constrained modulus of soils, stiffness parameters for the HSS model could be determined. According to Plaxis 3D manual (Brinkgreve *et al*. 2004), the power exponent "m" was in a range of 0.8~1.0 for fine-grained soils, and the range was 0.5~0.6 for coarse-grained soils. In addition, shear strain corresponding to initial shear modulus lay within a range of (1.0~3.5)×10^{-4}.

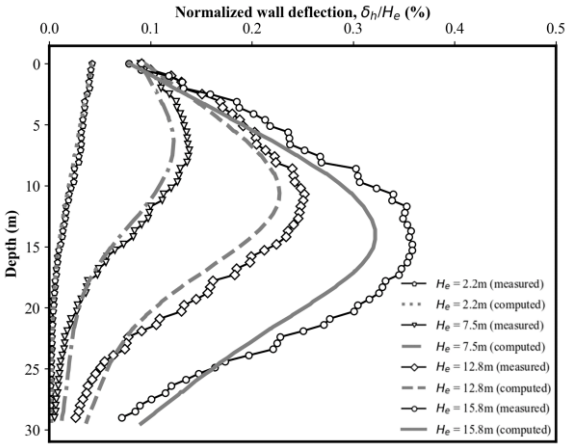

Fig. 4 Comparison of measured and computed lateral wall deflections due to basement excavation

3.4 Validation of soil model and model parameters

Fig. 4 compares the measured and computed lateral wall deflections due to basement excavation. Basement excavation-induced lateral wall deflections are normalized by the final excavation depth (i.e., H_e=15.8 m). Positive values denote retaining walls deflecting toward basement. When the excavation depth is 2.1 m, both measured and computed results show a cantilever-type wall deflection. This is because horizontal props have not been installed at this construction stage yet. However, deep-seated wall movements start to dominate as basement excavation proceeds to low depths. This is because the existence of concrete props constrains the lateral movements at the top of the retaining wall. The computed deflection shape of the retaining wall compares well with the monitored profile.

For the deep-seated wall movements, the location of maximum wall movement is closely related to excavation stages. When the excavation depths are 7.5, 12.8 and 15.8 m, corresponding measured maximum lateral wall movements are 0.14%H_e (21.8 mm), 0.25%H_e (39.8 mm) and 0.36% H_e (56.6 mm), which are only 10% larger than the computed results. Note that the discrepancies between the measured and computed lateral wall deflection increases as basement excavation goes deeper. This is properly due to the construction activities simulated in the numerical

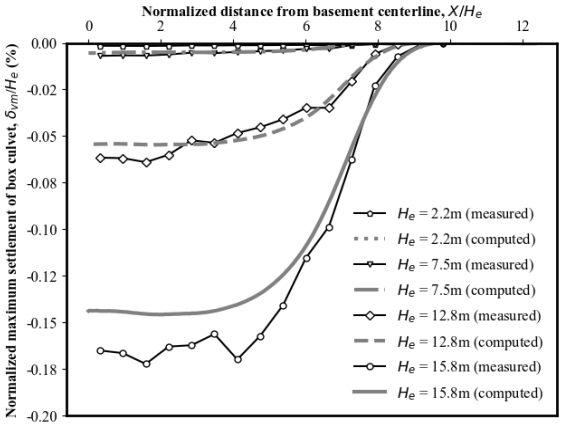

Fig. 5 Comparison of measured and computed settlements of box culvert

analysis are different from the field. There are surcharge and live loads surrounding the retaining wall in field. But those activities are not simulated in the numerical analysis. Thus, the computed lateral wall deflections are smaller than that measured in the field.

In general, the computed lateral wall movements have a good fit with measured results irrespective of excavation depths, which demonstrates that the calibrated constitutive soil model and associated soil parameters are suitable and accurate for predicting excavation-induced soil-structure interaction at this site.

Fig. 5 compares measured and computed settlements of the box culvert along its longitudinal direction. Negative values represent basement excavation-induced settlement of the box culvert. Because of unbalanced stress applied at both sides of the retaining wall, the wall deflects toward the excavated side. As expected, settlements are induced in soils behind the retaining wall. Accordingly, settlements are induced in the existing box culvert, which was located behind the retaining wall. As basement excavation goes further, settlements induced in the box culvert increase rapidly. Note that the maximum box settlement occurs at the basement centerline, and the box settlement decreases dramatically with increasing normalized distance from the basement centerline. As basement excavations approach the final excavation level, an increase in the discrepancies between measured and computed settlements of the existing box culvert is observed. This is consistent with the discrepancies between the computed and measured lateral wall deflection. The enlarged discrepancies between the measured and computed settlements of box culvert are also due to inconsistent construction activities in the numerical analysis and field.

At a normalized distance X of less than 4 H_e, the maximum differences between the measured and computed box settlements are less than 15%. Broadly speaking, the computed settlements of the box culvert are in good agreement with the measured results. The consistency between the measured and computed results implies that the adopted numerical modelling procedures and soil parameters are reasonable.

4. Three-dimensional numerical parametric study

4.1 Numerical analysis program

After validating the soil model and model parameters, a series of numerical parametric study was conducted to investigate systematically and comprehensively the complex basement-box culvert interaction. As the box culvert was in close proximity to the excavation, behavior of the box culvert is expected to be affected greatly by excavation geometry, relative position between basement and box culvert, and stiffness of retaining wall.

Table 4 summaries the numerical analysis program in this study. In total, 69 numerical analyses were carried out to investigated three-dimensional responses of the box culvert due to adjacent basement excavation in clays. More specifically, the normalized excavation length (L/H_e) and width (B/H_e) were designed to vary with a large range, namely, 2.0~15.8 and 2.0~10.0, respectively, in order to explore three-dimensional deformation mechanisms of the box culvert. All the basement geometries considered in this study were common values in practice (Shi *et al*. 2015b). To obtain the primary influence zone of box culvert settlement due to basement excavation, the normalized clear distance between the retaining wall and box culvert (h/H_e) varied between 0.25 to 2.0, and the normalized cover depth of box culvert ranged from 0.15 to 1.6. In addition, the designed

Table 4 Numerical analysis program of basement-soil-box culvert interaction

Parameters	Excavation length, L/H_e	Excavation width B/H_e	Distance between box and basement, h/H_e	Cover depth of box, C/H_e	Wall thickness, w (m)	Prop dimension (m)	Prop spacing, S (m)	Isolation wall
Excavation geometry	2.0 to 15.8	2.0 to 10.0	0.65	0.15	0.8	0.7×0.7	5.3	No
Basement-box relative position	15.8	8.2	0.25 to 2.0	0.15	0.8	0.7×0.7	5.3	No
Cover depth	15.8	8.2	0.65	0.15~ 1.6	0.8	0.7×0.7	5.3	No
Wall thickness	15.8	8.2	0.65	0.15	0.3 to 1.2	0.7×0.7	5.3	No
Prop dimension	15.8	8.2	0.65	0.15	0.8	0.7×0.7 to 1.2×1.2	5.3	No
Prop spacing	15.8	8.2	0.65	0.15	0.8	0.7×0.7	3.0, 4.0, 5.3	No
Isolation wall	15.8	8.2	0.65	0.15	0.8	0.7×0.7	5.3	Yes

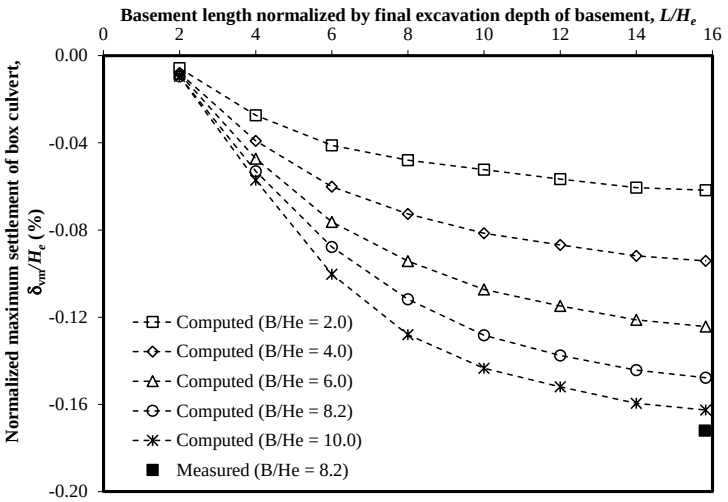

Fig. 6 Effects of excavation geometry on normalized maximum settlement of box culvert

thickness of retaining wall was in a range of 0.3 to 1.2 m in order to evaluate the effect of retaining system stiffness on the adjacent box culvert. The retaining wall with a thickness of 0.3 was corresponding to a typical sheet pile in field, and 1.2 m was a typical thickness of a diaphragm wall constructed in soft ground (Tan and Li 2011). Moreover, props with typical cross sections (i.e., 0.7 m×0.7 m to 1.2 m×1.2 m) and three vertical spacings (i.e., 3.0 m, 4.0 m, 5.3 m) were considered in the numerical analysis (Tan and Li 2011). One more numerical analysis was conducted to evaluate the effectiveness of isolation wall in reducing settlement of the box culvert.

5. Interpretation of computed results

5.1 Effects of excavation geometry on maximum movements of box culvert

Fig. 6 shows variations of the normalized maximum settlement of box culvert (δ_{vm}/H_e) along basement center with excavation length (L/H_e) and width (B/H_e). At a given excavation width, the basement excavation-induced maximum settlement in the box culvert increases with increasing excavation length, but at a reduced rate. It is anticipated that the curve will eventually become flat, and any further increase in the excavation length will not cause any difference in the settlement of box culvert. This is because at a certain excavation length, the whole three-dimensional excavation problem evolves to a plan strain condition, which is not affected by the excavation length. It is noted that the settlement of the box culvert located at the side of the basement is affected significantly by the lateral wall deflection, particularly when the excavation length ratio (L/H_e) is less than 8.0. This is attributed to the fact that the well-known "corner effects" has a diminished impact on restraining lateral wall movements when the excavation length increases beyond a certain limit (Lee *et al*. 2008).

By increasing the excavation length from 14 H_e to 16 H_e, the increase in the maximum settlement of the box culvert is less than 2.5% irrespective of the excavation width. In other words, the basement-soil-box culvert interaction along the basement centerline can be simplified as a two-dimensional plane strain condition when the excavation length is more than 14 H_e. In comparison, when the excavation length increases from 2 H_e to 14 H_e, excavation-induced maximum settlements under various excavation widths are shown to increase by 9.5~15.7 times. It is demonstrated that excavation geometry has a significant effect on adjacent box culvert in close proximity, which essentially agrees with observations of Hsiung *et al*. (2018). In practice, it is not uncommon to excavate basements with excavation lengths less than 2 H_e in close proximity to existing tunnels (e.g., Huang *et al*. 2014). If the basement-box culvert interaction along the centerline of a short excavation (i.e., L/H_e=2.0) is assumed falsely as a plane strain condition (i.e., L/H_e=12.0), the basement excavation-induced settlement in box culvert can be significantly overestimated, resulting in an overconservative and uneconomic design.

Similarly, the basement excavation-induced maximum settlement in the box culvert increases with increasing excavation width at a given excavation length, but at a reduced rate. When the excavation length is 14 H_e, the maximum settlement of box culvert increases by 1.63 times as the excavation width varies from 2 H_e to 10 H_e. Clearly, the excavation width of a basement also has great effects on deformation mechanisms of the box culvert. As the excavation width increase, much larger stress relief occurred within basement.

Aside from settlements, basement excavation can also induce horizontal movement in box culvert. Fig. 7 shows variations of the normalized maximum horizontal movement of box culvert (d_{hm}/H_e) along the basement centerline with excavation length (L/H_e) and width (B/H_e). It is found that basement exaction-induced maximum horizontal movements share similar patterns with the induced maximum vertical settlements (see Fig. 5) but with dramatically smaller magnitudes. As an increase in the excavation length or excavation width, the maximum horizontal movements of box culvert also increase, but at a reduced rate. As the normalized excavation length varies

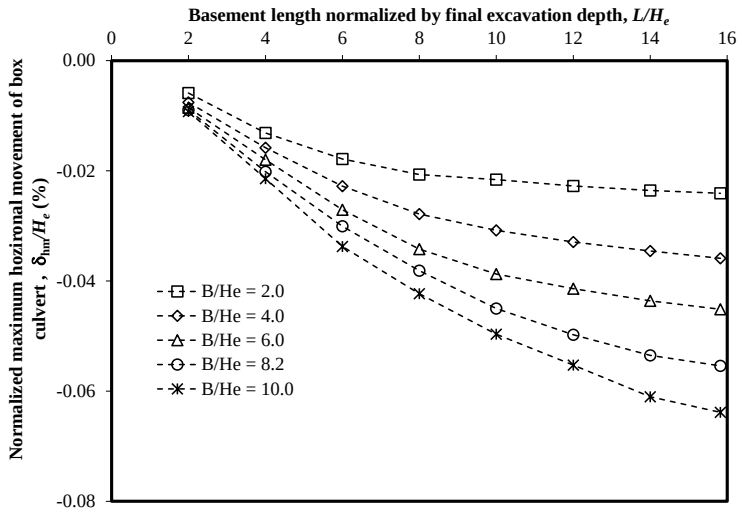

Fig. 7 Effects of excavation geometry on normalized maximum horizontal movement of box culvert

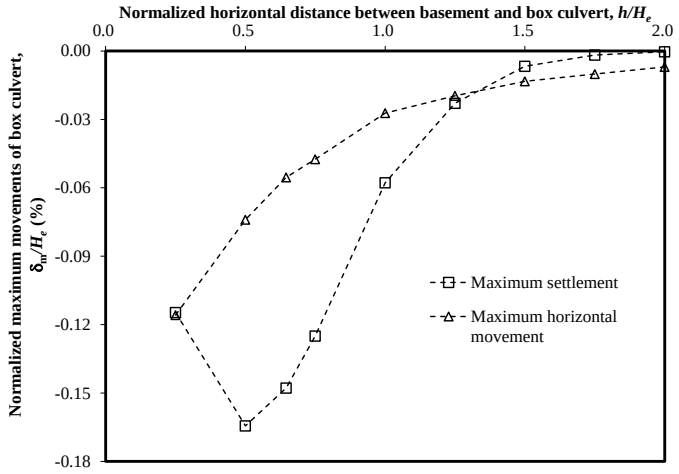

Fig. 8 Effects of clear distance between box culvert and retaining wall on settlement and horizontal movement of box culvert

from 14 H_e to 16 H_e, the increase in the maximum horizontal movements of box culvert under various excavation widths is less than 4.0%. Therefore, it is reasonable to conclude that the basement-box culvert interaction along the basement centerline can be considered as a plane strain problem when the excavation length reaches 14 H_e.

By simplifying a short basement-box interaction (i.e., L/H_e=2.0) as a plane strain condition (i.e., L/H_e=12.0), the maximum horizontal movements of the box culvert are overestimated by 3.0~5.1 times. Three-dimensional analyses are thus required to precisely simulate excavation geometries in order to obtain an accurate estimation of box culvert deformations. Otherwise, deformation of box culvert is grossly overestimated by conducting two-dimensional numerical analysis of basement-box culvert interaction. Since the excavation length has substantial effects on the performance of adjacent box culvert, countermeasures such as installation of partition wall or stagger excavation method are recommended to ensure serviceability of existing box culvert, which is discussed in the coming subsection 5.7.

5.2 Effects of clear distance between box culvert and retaining wall on box settlement and lateral movement

Fig. 8 shows variations of box culvert deformations with clear distance (h) between the box culvert and retaining wall. The computed maximum settlement and horizontal movements at the end of basement excavation are presented. Vertical settlement and horizontal deflection towards excavation are presented as negative values. As the clear distance between the box culvert and retaining wall increases, the basement excavation-induced maximum settlement in the box culvert is shown to increases first, followed by a rapid decrease. More specifically, it is found that the maximum settlement (i.e., 0.16% H_e) of the box culvert occurs at a normalized clear distance of 0.5 H_e. The concave-shaped ground settlement profile is induced by the basement excavation, which corresponds to the deep-seated wall deflection profile as shown in Fig. 4.

In contrast, the maximum horizontal movement of the box culvert monotonically deceases as the clear distance between the box culvert and basement increases. By varying the clear distance from 0.16 H_e to 1.5 H_e, the

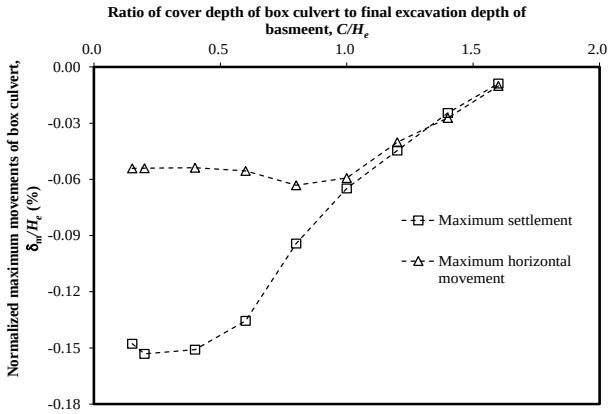

Fig. 9 Effects of cover depth of box culvert on its settlement and horizontal movement

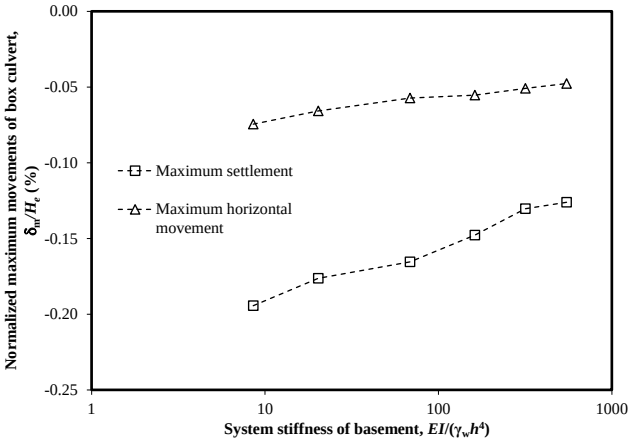

Fig. 10 Effects of flexural stiffness of retaining wall on box culvert settlement and horizontal movement

basement excavation-induced maximum settlement and horizontal movement are reduced by 95.9% and 88.5%, respectively. When the normalized clear distance is 2 H_e, the basement excavation-induced maximum settlement of the box culvert is close to zero, and the maximum horizontal movement of the box culvert is as small as 0.007% H_e (i.e., 1.1 mm). Therefore, it is reasonable to conclude that the major influence zone of the box culvert deformations due to adjacent basement excavation is 1.5 times of the final excavation depth (i.e., 1.5 H_e). For box culvert buried within this region, special attentions should be paid to the additional deformations induced by basement excavation. Extra strengthening measures should be implemented if the box culvert or any other infrastructures (e.g., tunnels and pipelines) in close proximity are sensitive to vertical and horizontal deformations.

5.3 Effects of cover depth of box culvert on its settlement and horizontal movement

Fig. 9 shows variations of the maximum settlement and horizontal movement with cover depth of the box culvert. When the cover depth is less than 0.4 H_e, the basement excavation-induced settlement of the box culvert is almost unaffected by the burial depth of box culvert. When the cover depth is larger than 0.4 H_e, the maximum settlement of box culvert decreases rapidly as an increase in the cover depth. When the normalized cover depth (C/H_e) reaches 1.6, the maximum settlement of the box culvert is as small as 0.0088% H_e (i.e., 1.4 mm).

The box culvert exhibits a totally different horizontal deformation pattern with an increase in the burial depth of the box culvert as compared with that for the vertical settlement. Essentially, the magnitude of the computed maximum horizontal displacement is about half of that for the computed vertical settlement. More importantly, the maximum horizontal movement is less sensitive to the variation of the cover depth of the box culvert. Although it is found that the horizontal movement increases slightly first at C/H_e<0.8, followed by a rapid decrease when the cover depth ratio increases beyond 0.8 (i.e., C/H_e>0.8). The computed maximum horizontal distance remains relatively stable, and a large decrement occurs when the cover depth increases beyond 1.0 (i.e., C/H_e=1.0). In comparison, significant variations of the maximum vertical settlement initiate at C/H_e=0.6. It is also found that the maximum horizontal movement of 0.063% H_e (i.e., 9.98 mm) is observed at C=0.8 H_e, which is essentially coincident with the location of the maximum lateral wall movement as shown in Fig. 4. When the normalized cover depth (C/H_e) increases to 1.6, the maximum horizontal movement induced in the box culvert is only 0.01% H_e (i.e., 1.58 mm). It is indicated that the effects of basement excavation on the box culvert are negligible when the box culvert is located at 0.6 H_e below the formation level of basement.

5.4 Effects of flexural stiffness of retaining wall on settlement and horizontal movement of box culvert

It is widely acknowledged that the removal of soil mass during excavation can impose unbalanced earth pressures on both sides of a retaining structure and lead to lateral wall deflections. The key factor governing the lateral wall deflection of an excavation is the system stiffness (Liyanapathirana and Nishanthan 2016, Sun *et al*. 2019). More specifically, lateral wall deflections of an excavation are primarily governed by wall thickness, cross section of props and vertical spacing of props. In practice, sheet pile, bored pile and diaphragm walls are most commonly forms of retaining structures. Irrespective of the wall types, plate elements are typically adopted to model retaining structures. Therefore, effects of flexural wall stiffness can be explicitly investigated by varying thicknesses of a retaining wall. In this study, unit weight of water (γ_w) and averaged vertical spacing (S) are used to normalize the flexural stiffness (EI) of a retaining wall. For example, a system stiffness ($EI/(\gamma_w S^4)$) of 8.55 is equivalent to a typic U-shaped sheet pile wall (i.e., type NSP III with a moment of inertia of 3.24×10^{-4} m^4/m). In comparison, when the system stiffness of a wall is 547.5, it is equivalent to a concrete diaphragm wall with a thickness of 1.2 m. As summarized in Table 4, the variation in wall flexural stiffness is realized via a change in the wall thickness between 0.3 m and 1.2 m.

As shown in Fig. 10, the basement excavation-induced settlement and horizontal movement of the box culvert are

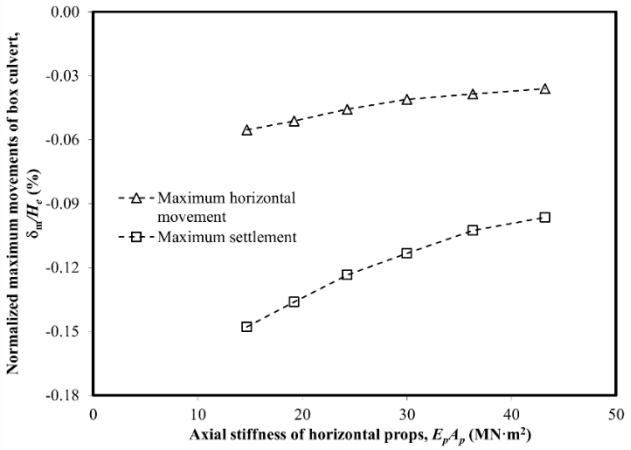

Fig. 11 Effects of axial stiffness of props on box culvert settlement and horizontal movement

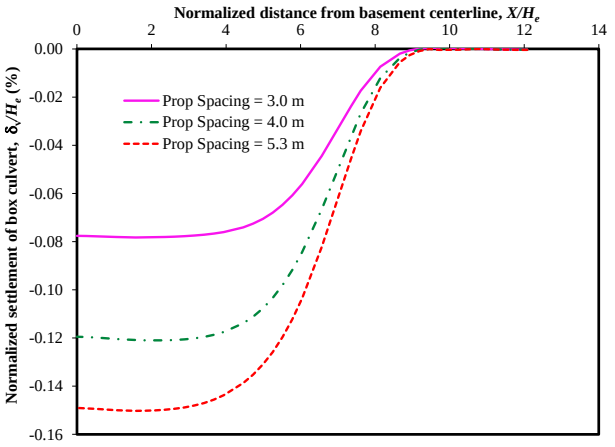

Fig. 12 Effects of vertical spacing of props on box settlement

shown to decrease monotonically with an increase in the system stiffness of basement (i.e., wall thickness). As the system stiffness increases from 8.55 (i.e., sheet pile wall) to 547.5 (i.e., 1.2 m thick diaphragm wall), the maximum settlement and horizontal movement of the box culvert are reduced by 35.1% and 36.0%, respectively. This is because a stiffer wall has a larger bending capacity to prevent potential excessive deflections toward basement.

5.5 Effects of axial stiffness of props on box culvert settlement and horizontal movement

Fig. 11 shows variations of maximum settlement and horizontal movement of the box culvert with increasing axial stiffness of props. Similarly, axial stiffness is a product of cross-sectional area (A_p) and Young's Modulus (E_p). Therefore, a variation in axial stiffness can be simplified as a change in the total cross-sectional area. Props are square in cross section, whose dimension varied between 0.7 m×0.7 m and 1.2 m×1.2 m. It can be seen that both the computed maximum settlement and horizontal movement of the box culvert exhibit a monotonic reducing trend with an increase in the axial stiffness. This is as expected because props with a larger cross section can better sustain a given axial force at a smaller axial compression during basement excavation. Accordingly, the lateral movements of retaining wall are reduced, and the active earth pressure behind the retaining wall is maintained, leading to small variations in the computed maximum settlement and horizontal movement of the box culvert. More specifically, by increasing the axial stiffness of props (E_pA_p) from 14.7 MN·m^2 (i.e., cross section of 0.7 m×0.7 m) to 43.2 MN·m^2 (i.e., cross section of 1.2 m×1.2 m), the maximum settlement and horizontal movement induced in the box culvert are reduced by 34.7% and 35.0%, respectively. It is also worth mentioning that increasing the axial stiffness of props have similar effects as that of enhancing flexural stiffness of retaining wall (see Fig. 10). Both factors result in a monotonic reduction in the computed settlement and horizontal movement of the box culvert with increasing stiffness. Note that conventional excavation support systems mainly quantify the effects of support spacing and wall bending stiffness on excavation performance (Bryson *et al*. 2012) and pays much less attention to the axial stiffness of props. Results in Fig. 11 highlights the importance of considering axial stiffness of props in controlling deformations of the existing box culvert in addition to adjustments of conventional stiffness factors such as support spacing and wall flexural stiffness.

5.6 Effects of vertical spacing of props on box settlement

Fig. 12 shows variations of the basement excavation-induced longitudinal settlement in box culvert with vertical spacing of props. Note that vertical spacing (S) of props can significantly affect the overall retaining system stiffness, which is proportional to the reciprocal of the four-order of the vertical spacing (i.e., $EI/(\gamma_w S^4)$). As the vertical spacing of props is reduced, the system stiffness of retaining structures increases dramatically, which results in an obvious reduction in the maximum settlement of the box culvert. By decreasing the vertical spacing of props from 5.3 m to 4.0 and 3.0 m, the maximum settlements of the box culvert are reduced by 19.9% and 48.0%, respectively. Obviously, props with a small vertical spacing can effectively strengthen the retaining system and reduce settlements of the box culvert due to adjacent basement excavation.

It is also observed that the computed settlement of the box culvert remains relatively stable at a normalized distance of 0~4 H_e from the basement centerline irrespective of the vertical spacing. In other words, the maximum settlement of the box culvert can be calculated by simply carrying out a two-dimensional analysis. However, when the distance from the basement centerline increases further, there is a rapid reduction in the computed box culvert settlement. It is also worth noting that angular distortion induced by different settlements along the longitudinal direction is a key factor governing serviceability of structures. For the box culvert in this study, the calculated maximum angular distortion is about 0.6 mm/m at a vertical spacing of 5.3 m, and the value remains well below a nominal criterion of 1 mm/m. The maximum

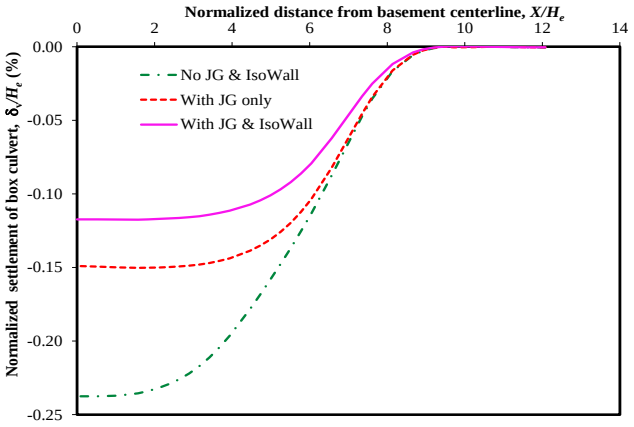

Fig. 13 Effects of jet grouting and isolation wall on settlement of box culvert

angular distortion greatly diminishes when the vertical spacing reduces. In practice, engineers prefer to oversimplifying a three-dimensional excavation problem as a plan strain condition due to its simplicity and convenience for implementation. However, this practice normally can only give an overall maximum settlement without informing about the potential differential settlement pattern, which is considered critical for assessing serviceability of sensitive infrastructures such as water pipelines.

5.7 Effects of jet grouting and isolation wall on settlements of box culvert

For excavations in soft ground or locations with sensitive infrastructures, it is conventional to implement ground improvement measures such as jet grouting columns or other countermeasures such as isolation wall. For example, the installation of jet grouting columns within the excavation site can improve strength and stiffness of soils in the passive side. Similarly, the construction of isolation wall behind a retaining structure can assist in strengthening the ground and reduce the stress propagation to nearby sensitive structures. In this study, the effectiveness of both common strengthening measures (i.e., jet grouting columns and isolation wall) are explicitly modelled in the numerical analysis to evaluate the effectiveness in reducing deformations of the existing box culvert. Since responses of the box culvert are greatly affected by upper fill, soft clay and silty clay layers, the isolation wall is proposed to penetrate through those three layers with a total depth of 24.0 m. Moreover, the isolation wall is modelled at 13.5 m away from the retaining wall. Cross walls are constructed to connect with the retaining wall to improve the integrity of the retaining system. The stiffness and strength parameters of jet grouting and isolation are shown in Table 3. The thickness of the isolation wall simulated in this study is 0.7 m.

Fig. 13 shows variations of basement excavation-induced settlements in the existing box culvert considering different ground strengthening schemes. It is found that the basement excavation-induced maximum settlement of the box culvert is 0.24% H_e without implementing any ground improvement measure. After installing jet grouting columns inside the excavation site, the passive soil resistance in front of the retaining wall improves. Accordingly, the basement excavation-induced maximum settlement in the box culvert becomes 0.15% H_e (i.e., decreased by 37.2%). In comparison, by constructing an isolation wall in between the retaining wall and box culvert, the computed maximum settlement of the box culvert reduces to 0.12% H_e.

As shown in Table 3, the stiffness of cement soil is much higher than that of soil. By installation of insulation wall with large stiffness, soil movements behind the retaining wall are suppressed. Consequently, deformation of the existing box culvert due to basement is reduced. Clearly, the maximum settlement of the box culvert is reduced by 50.6% if both jet grouting columns and the isolation wall are implemented. In other words, the isolation wall can help reduce the maximum settlement of the box culvert by 13.4%. Therefore, it is reasonable to conclude that jet grouting columns is more effective in reducing the box culvert settlement than the isolation wall in this study. In order to minimize excavation effects on adjacent sensitive structures, it is recommended to reinforce the ground by installing jet grouting columns.

6. Conclusions

In this study, a series of three-dimensional numerical analyses was conducted to investigate deformation characteristics of a box culvert due to an adjacent basement excavation in clays. Effects of basement geometry, relative position between box culvert and basement, system stiffness of basement and countermeasures on culvert deformations were explored. Field measurements were adopted to calibrate soil model and associated model parameters. Based on the computed results, the following conclusions may be drawn:

- Basement excavation-induced maximum settlements of the box culvert are found to increase with excavation length or excavation width, but at a reduced rate. When the excavation length reaches 14 H_e (i.e., final excavation depth), the basement-box culvert interaction along the basement centerline can be considered as a plane strain condition.
- If the basement-box culvert interaction along the centerline of a short excavation (i.e., L/H_e=2.0) is falsely simplified as a plane strain condition (i.e., L/H_e=12.0), the maximum settlements and horizontal movements of the box culvert are overestimated by 9.5~15.7 times and 3.0~5.1 times, respectively. In order to have a reasonable estimation of culvert deformations, excavation geometry should be precisely simulated in three-dimensional numerical analyses.
- For the multi-propped basement excavation simulated in this study, the major influence zone of box culvert deformations due to adjacent basement excavation is 1.5 times of the final excavation depth (i.e., 1.5 H_e). Moreover, the effects of basement excavation on box culvert are negligible when the box culvert is located 0.6 H_e below the formation level of basement.

• Basement excavation-induced maximum movements of the box culvert are reduced by up to 36.0%, when a 1.2 m thick diaphragm wall is adopted instead of a sheet pile wall. By increasing the cross section of props from 0.7 m×0.7 m to 1.2 m×1.2 m, the maximum movements of the box culvert are reduced by up to 35.0%. In addition, the maximum movements of the box culvert are reduced by 48% when the vertical spacing of props is decreased from 5.3 m to 3.0 m.
• It is found that jet grouting of soil within the basement and installation of isolation wall can effectively reduce basement excavation-induced movements in the adjacent box culvert. Compared with the maximum settlement of the box culvert without any countermeasures, jet grouting and installation of isolation wall can reduce the maximum settlement of box culvert by 37.2% and 13.4%, respectively. Obviously, the use of jet grouting on reducing movements of box culvert are much more prominent than an isolation wall.

References

Ardakani, A., Bayat, M. and Javanmard, M. (2014), "Numerical modeling of soil nail walls considering Mohr Coulomb, hardening soil and hardening soil with small-strain stiffness effect models", *Geomech. Eng.*, **6**(4), 391-401. https://doi.org/10.12989/gae.2014.6.4.391.

Brinkgreve, R.B.J. and Broere, W. (2004), PLAXIS 3D Tunnel Version 2, PLAXIS by, Netherlands.

Bryson, L.S. and Zapata-Medina, D.G. (2012). "Method for estimating system stiffness for excavation support walls", *J. Geotech. Geoenviron. Eng.*, **138**(9), 1104-1115. https://doi.org/10.1061/(ASCE)GT.1943-5606.0000683.

Devriendt, M., Doughty, L., Morrison, P. and Pillai, A. (2010), "Displacement of tunnels from a basement excavation in London", *Proc. Inst. Civil Eng.-Geotech. Eng.*, **163**(3), 131-145. https://doi.org/10.1680/geng.2010.163.3.131.

Fang, J.C., Kong, G.Q. and Yang, Q. (2022), "Group performance of energy piles under cyclic and variable thermal loading", *J. Geotech. Geoenviron. Eng.*, **148**(8), 04022060. https://doi.org/10.1061/(ASCE)GT.1943-5606.0002840.

Fong, F.H., Standing, J.R. and Bourne-Webb, P.J. (2014), "Building response to adjacent deep basement construction", *Proc. Inst. Civil Eng.-Geotech. Eng.*, **167**(2), 130-143. https://doi.org/10.1680/geng.13.00051.

Hsieh, P.G. and Ou, C.Y. (1998), "Shape of ground surface settlement profiles caused by excavation", *Can. Geotech. J.*, **35**(6), 1004-1017. https://doi.org/10.1139/cgj-35-6-1004.

Hsiung, B.C.B., Yang, K.H., Aila, W. and Ge, L. (2018), "Evaluation of the wall deflections of a deep excavation in Central Jakarta using three-dimensional modeling", *Tunnel. Undergr. Space Technol.*, **72**, 84-96. https://doi.org/10.1016/j.tust.2017.11.013.

Huang, X., Huang, H.W. and Zhang, D.M. (2014), "Centrifuge modelling of deep excavation over existing tunnels", *Proc. ICE-Geotech. Eng.*, **167**(2), 3-18. https://doi.org/10.1680/geng.11.00045.

Kouretzis, G.P., Krabbenhøft, K., Sheng, D. and Sloan, S.W. (2014), "Soil-buried pipeline interaction for vertical downwards relative offset", *Can. Geotech. J.*, **51**(10), 1087-1094. https://doi.org/10.1139/cgj-2014-0029.

Lee, F.H., Yong, K.Y., Quan, K.C. and Chee, K.T. (1998), "Effect of corners in strutted excavations: Field monitoring and case histories", *J. Geotech. Geoenviron. Eng.*, **124**(4), 339-349. https://doi.org/10.1061/(ASCE)1090-0241(1998)124:4(339).

Liyanapathirana, D.S. and Nishanthan, R. (2016), "Influence of deep excavation induced ground movements on adjacent piles", *Tunnel. Undergr. Space Technol.*, **52**, 168-181. https://doi.org/10.1016/j.tust.2015.11.019.

Mu, L., Huang, M., Roodi, G.H. and Shi, Z. (2021), "Allowable wall deflection of braced excavation adjacent to pile-supported buildings", *Geomech. Eng.*, **26**(2), 161-173. https://doi.org/10.12989/gae.2021.26.2.161.

Ng, C.W., Shakeel, M., Wei, J. and Lin, S. (2021), "Performance of existing piled raft and pile group due to adjacent multi-propped excavation: 3d centrifuge and numerical modelling", *J. Geotech. Geoenviron. Eng.*, **147**(4), 04021012. https://doi.org/10.1061/(ASCE)GT.1943-5606.0002501.

Ng, C.W.W., Hong, Y., Liu, G.B. and Liu, T. (2012), "Ground deformations and soil-structure interaction of a multi-propped excavation in Shanghai soft clays", *Géotechnique*, **62**(10), 907-921. https://doi.org/10.1680/geot.10.P.072.

Ng, C.W.W., Shi, J.W. and Hong, Y. (2013), "Three-dimensional centrifuge modelling of basement excavation effects on an existing tunnel in dry sand", *Can. Geotech. J.*, **50**(8), 874-888. https://doi.org/10.1139/cgj-2012-0423.

Ng, C.W.W., Simons, N. and Menzies, B. (2004), Soil-Structure Engineering of Deep Foundations, Excavations and *Tunnels*, Thomas Telford, UK.

Ng, C.W.W., Xu, J. and Yung, S.Y. (2009), "Effects of wetting-drying and stress ratio on anisotropic stiffness of an unsaturated soil at very small strains", *Can. Geotech. J.*, **46**(9), 1062-1076. https://doi.org/10.1139/T09-043.

Nguyen, T.S. and Likitlersuang, S. (2021). "Influence of the spatial variability of soil shear strength on deep excavation: A case study of a Bangkok underground MRT station", *Int. J. Geomech.*, **21**(2), 04020248. https://doi.org/10.1061/(ASCE)GM.1943-5622.0001914.

O'Rourke, T.D., Stewart, H.E. and Jeon, S.S. (2001), "Geotechnical aspects of lifeline engineering", *Proc. Inst. Civil Eng.-Geotech. Eng.*, **149**(1), 13-26. https://doi.org/10.1680/geng.2001.149.1.13.

Pan, Y., Liu, Y., Xiao, H., Lee, F.H. and Phoon, K.K. (2018), "Effect of spatial variability on short-and long-term behaviour of axially-loaded cement-admixed marine clay column", *Comput. Geotech.*, **94**, 150-168. https://doi.org/10.1016/j.compgeo.2017.09.006.

Qian, J., Tong, Y., Mu, L., Lu, Q. and Zhao, H. (2020), "A displacement controlled method for evaluating ground settlement induced by excavation in clay", *Geomech. Eng.*, **20**(4), 275-285. https://doi.org/10.12989/gae.2020.20.4.275.

Shi, C. and Wang, Y. (2021), "Smart determination of borehole number and locations for stability analysis of multi-layered slopes using multiple point statistics and information entropy", *Can. Geotech. J.*, **58**(11), 1669-1689. https://doi.org/10.1139/cgj-2020-0327.

Shi, J.W., Chen Y.H., Lu, H., Ma, S.K. and Ng, C.W.W. (2022a), "Centrifuge modeling of the influence of joint stiffness on pipeline response to underneath tunnel excavation", *Can. Geotech. J.*, **59**(9), 1568-1586. https://doi.org/10.1139/cgj-2020-0360.

Shi, J.W., Ding C., Ng, C.W.W., Lu, H. and Chen L. (2020), "Effects of overconsolidation ratio on tunnel responses due to overlying basement excavation in clay", *Tunnel. Undergr. Space Technol.*, **7**, 103247. https://doi.org/10.1016/j.tust.2019.103247.

Shi, J.W., Fu, Z.Z. and Guo, W.L. (2019), "Investigation of geometric effects on three-dimensional tunnel deformation mechanisms due to basement excavation", *Comput. Geotech.*, **106**, 108-116. https://doi.org/10.1016/j.compgeo.2018.10.019.

Shi, J.W., Liu, G.B., Huang, P. and Ng, C.W.W. (2015a), "Interaction between a large triangular excavation and adjacent structures in Shanghai soft clay", *Tunnel. Undergr. Space Technol.*, **50**, 282-295. https://doi.org/10.1016/j.tust.2015.07.013.

Shi, J.W., Ng, C.W.W. and Chen, Y.H. (2015b), "Three-dimensional numerical parametric study of the influence of basement excavation on existing tunnel", *Comput. Geotech.*, **63**, 146-158. https://doi.org/10.1016/j.compgeo.2014.09.002.

Shi, J.W., Wei, J.Q., Ng, C.W.W., Lu, H. Ma, S.K., Shi, C. and Li P. (2022b), "Effects of construction sequence of double basement excavations on an existing floating pile", *Tunnel. Undergr. Space Technol.*, **119**, 104230. https://doi.org/10.1016/j.tust.2021.104230.

Shi, J.W., Zhang, X., Chen, Y. and Chen, L. (2018), "Numerical parametric study of countermeasures to alleviate basement excavation effects on an existing tunnel", *Tunnel. Undergr. Space Technol.*, **72**, 145-153. https://doi.org/10.1016/j.tust.2017.11.030.

Soomro, M.A., Saand, A., Mangi, N., Mangnejo, D.A., Karira, H. and Liu, K. (2021), "Numerical modelling of effects of different multipropped excavation depths on adjacent single piles: comparison between floating and end-bearing pile responses", *Eur. J. Environ. Civil Eng.*, **25**(14), 2592-2622. https://doi.org/10.1080/19648189.2019.1638312.

Sun, H., Chen, Y., Zhang, J. and Kuang, T. (2019), "Analytical investigation of tunnel deformation caused by circular foundation pit excavation", *Comput. Geotech.*, **106**, 193-198. https://doi.org/10.1016/j.compgeo.2018.11.001.

Tan, Y. and Li, M.W. (2011), "Measured performance of a 26 m deep top-down excavation in downtown Shanghai", *Can. Geotech. J.*, **48**(5), 704-719. https://doi.org/10.1139/T10-100.

Wang, W.D., Ng, C.W., Hong, Y., Hu, Y. and Li, Q. (2019), "Forensic study on the collapse of a high-rise building in Shanghai: 3D centrifuge and numerical modelling", *Géotechnique*, **69**(10), 847-862. https://doi.org/10.1680/jgeot.16.P.315.

Wang, Y., Shi, C. and Li, X. (2022), "Machine learning of geological details from borehole logs for development of high-resolution subsurface geological cross-section and geotechnical analysis", *Georisk*, **16**(1), 2-20. https://doi.org/10.1080/17499518.2021.1971254.

Wong, K.S., Mašín, D. and Ng, C.W.W. (2014), "Modelling of shear stiffness of unsaturated fine grained soils at very small strains", *Comput. Geotech.*, **56**, 28-39. https://doi.org/10.1016/j.compgeo. 2013.10.005.

Yang, Y., Li, J., Liu, C., Ma, J., Zheng, S. and Chen, W. (2022), "Influence of deep excavation on adjacent bridge piles considering underlying karst cavern: A case history and numerical investigation", *Acta Geotechnica*, **17**(2), 545-562. https://doi.org/10.1007/s11440-021-01213-w.

Zhang, Q.Q., Liu, S.W., Feng, R.F. and Li, X.M. (2019), "Analytical method for prediction of progressive deformation mechanism of existing piles due to excavation beneath a pile-supported building", *Int. J. Civil Eng.*, **17**(6), 751-763. https://doi.org/10.1007/s40999-018-0309-9.

Zheng, G., Yang, X.Y., Zhou, H.Z., Du, Y.M., Sun, J.Y. and Yu, X.X. (2018), "A simplified prediction method for evaluating tunnel displacement induced by laterally adjacent excavations," *Comput. Geotech.*, **95**, 119-128. https://doi.org/10.1016/j.compgeo.2017.10.006.